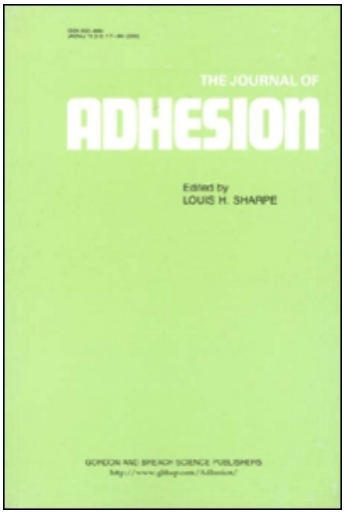

The Journal of Adhesion
Publication details, including instructions for authors and subscription information:
http://www.informaworld.com/smpp/title~content=t713453635

A Comparison of the Prediction of Fatigue Damage and Crack Growth in Adhesively Bonded Joints Using Fracture Mechanics and Damage Mechanics Progressive Damage Methods

I. A. Ashcroft[a]; V. Shenoy[a]; G. W. Critchlow[b]; A. D. Crocombe[c]
[a] Wolfson School of Mechanical and Manufacturing Engineering, Loughborough University, United Kingdom [b] Materials Engineering, Loughborough University, United Kingdom [c] School of Engineering, University of Surrey, Guildford, Surrey, United Kingdom

Online publication date: 01 December 2010

To cite this Article Ashcroft, I. A. , Shenoy, V. , Critchlow, G. W. and Crocombe, A. D.(2010) 'A Comparison of the Prediction of Fatigue Damage and Crack Growth in Adhesively Bonded Joints Using Fracture Mechanics and Damage Mechanics Progressive Damage Methods', The Journal of Adhesion, 86: 12, 1203 — 1230
To link to this Article: DOI: 10.1080/00218464.2010.529383
URL: http://dx.doi.org/10.1080/00218464.2010.529383

The Journal of Adhesion, 86:1203–1230, 2010

ISSN: 0021-8464 print/1545-5823 online
DOI: 10.1080/00218464.2010.529383

Taylor & Francis
Taylor & Francis Group

A Comparison of the Prediction of Fatigue Damage and Crack Growth in Adhesively Bonded Joints Using Fracture Mechanics and Damage Mechanics Progressive Damage Methods

I. A. Ashcroft[1], V. Shenoy[1], G. W. Critchlow[2] and A. D. Crocombe[3]
[1]Wolfson School of Mechanical and Manufacturing Engineering, Loughborough University, United Kingdom
[2]Materials Engineering, Loughborough University, United Kingdom
[3]School of Engineering, University of Surrey, Guildford, Surrey, United Kingdom

Lifetime prediction of adhesively bonded joints under constant amplitude fatigue has been carried out using two finite element-based, progressive damage modelling methods. The first method used a fracture mechanics (FM)-based crack growth law in which the relationship between strain energy release rate and crack growth rate under fatigue was determined from experiments using compound double cantilever beam specimens. It was found that the FM approach predicted the fatigue life well at higher fatigue loads but under-predicted the fatigue life at lower fatigue loads. This was attributed to the increasing importance of crack initiation at lower fatigue loads. This problem was solved in the second predictive method, which was based on a continuum damage mechanics approach. A power law relationship to plastic strain was used to define the damage rate. The damage law was able to simulate damage evolution prior to crack growth and excellent predictions of fatigue life were found at all fatigue loads.

Keywords: Damage mechanics; Fatigue; Fracture mechanics; Plastic strain

Received 23 December 2009; in final form 24 August 2010.
One of a Collection of papers honoring David A. Dillard, the recipient in February, 2010 of *The Adhesion Society Award for Excellence in Adhesion Science, Sponsored by 3M*.
Address correspondence to I. A. Ashcroft, Wolfson School of Mechanical and Manufacturing Engineering, Loughborough University, Loughborough, Leicestershire LE11 3TU, UK. E-mail: i.a.ashcroft@lboro.ac.uk

1. INTRODUCTION

The use of adhesive bonding as a joining method and for patch repairs is increasing in many industries. The many advantages, including: high strength to weight ratio, high stiffness, not having to drill holes in the structures, and low thermal effects, make bonded joints a good replacement for bolted, riveted, or welded joints in the aerospace, marine, construction, and automotive industries. Fatigue analysis of adhesive joints is important in these industries as this is the most significant form of loading. Fatigue crack initiation and propagation behaviour in bonded joints is dependent on a number of factors, including: the nature of the adhesive, the loading and environmental conditions, and the joint geometry. A number of fatigue lifetime prediction methods have been proposed for bonded joints, as recently reviewed by Ashcroft and Crocombe [1].

There are a number of ways in which fatigue lifetime can be predicted for materials in general [2]. Broadly, they can be classified as: total-life-based, Miner's rule-based, phenomenological, and progressive damage modelling. In the total-life approaches, fatigue life criteria are proposed using traditional stress-life (S-N) or Goodman-type diagrams. These diagrams are highly dependent on many factors, including: geometry and loading and environmental conditions, and do not provide information on the accumulation of damage. Whilst providing a useful characterisation of fatigue behaviour for a given system, these methods are of limited use in failure prediction.

The S-N curve is only directly applicable to constant amplitude fatigue, whereas in many cases variable amplitude fatigue spectra are experienced. A simple method to use S-N data to predict variable amplitude fatigue was proposed by Palmgren [3], and then further developed by Miner [4], based on a linear accumulation of damage. However, there are a number of serious limitations to this method. It is assumed that damage accumulation is linear and that there is no load history effect, which is not necessarily the case for bonded joints. It is assumed that cycles below the fatigue limit will not contribute to the damage accumulation; however, once a crack has formed by the action of stresses above the fatigue limit then it may continue to propagate at stresses below the fatigue limit. This can be accounted for in a modified Palmgren-Miner (P-M) rule; however, Erpolat *et al.* [5] showed that even in this case the lifetime of bonded double lap joints subjected to variable amplitude fatigue was severely overestimated. This is the opposite trend to that frequently seen in metals, where it is seen that an overload can induce crack root plasticity, which retards crack growth, leading to under-predictions of fatigue life using the P-M rule.

Phenomenological models relate fatigue failure to measureable phenomena, such as the reduction in strength or stiffness during fatigue loading. A strength wearout approach can be used, in a modified form, to predict the fatigue life of composites [6] and bonded joints [5] subjected to variable amplitude fatigue. Whilst this method has the advantage over the total life approach in representing the progressive reduction in strength with fatigue cycling, it is similarly dependent on intensive testing using samples applicable to the application in question. Another drawback of this approach is that the form of degradation in many cases must be assumed because of the difficulty in correlating reduction in strength or stiffness to damage during fatigue loading. A more physically meaningful prediction of the fatigue failure process can be obtained through the use of progressive damage models (PDM).

PDM can be based on fracture mechanics (FM) or damage mechanics (DM) approaches. In the FM approach, a fracture parameter such as the stress intensity factor (K) or strain energy release rate (G) is used as the criterion for crack growth. The selected fracture parameter is usually related to the fatigue crack growth rate through a logarithmic plot and a curve fit to the plotted data is used to determine an empirical crack growth law. Finite element analysis (FEA), or closed form analysis in some cases, can be used to determine the fracture parameter as a function of crack length for a particular joint and the crack growth rate determined from the crack growth law. Numerical crack growth integration can then be used to predict crack growth and the number of cycles to failure. For example, in the case of bonded joints, G was used to predict the fatigue lifetime by Abdel Wahab *et al.* [7] by implementing the numerical crack growth integration into a FEA subroutine. Erpolat *et al.* [5] used a similar approach to predict the lifetime of bonded joints subjected to variable amplitude fatigue, and noted crack acceleration after overloads. A method of modelling this behaviour was proposed by Ashcroft [8], wherein, a damage shift factor was used to simulate load interaction effects. Nevertheless, the basic drawback of using FM modelling is that it does not involve the crack initiation process. This can result in an under-prediction of the fatigue life, especially in cases where crack initiation dominates the fatigue life. For example, Shenoy *et al.* [9] found that, for bonded joints at low fatigue loads, most of the fatigue lifetime is spent in crack initiation rather than crack propagation. One method of accounting for the initiation period is by determining a relationship between the number of cycles to initiation and a suitable parameter, such as the singularity parameter proposed by Lefebvre and Dillard [10]. This

approach was combined with a fracture mechanics approach to provide a whole life prediction method by Quaresimin and Ricotta [11].

The approach described above requires two separate analyses to predict the initiation and propagation lives and is, hence, demanding with respect to analysis and experimentation. Moreover, there is no indication of damage evolution in the initiation phase or damage other than the dominant crack in the propagation phase. A potentially more economic and physically meaningful method of whole life fatigue modelling is through a damage mechanics (DM) crack initiation approach in which the evolution of damage initiation prior to crack growth is simulated. This approach has been used for both metals and composite materials, for both quasi-static and fatigue loading [12,13]. However, modelling damage using this approach requires many constants to be defined or determined through experiments. Abdel Wahab *et al.* [14] provided a comparison of FM and DM approaches to predict the fatigue lifetime of bonded joints.

In this paper, both FM- and DM-based approaches are used to predict the fatigue lifetime of bonded lap joints under constant amplitude fatigue (CAF). In the first part of the paper, experimental results from FM experiments using compound double cantilever beam (CDCB) specimens and fatigue tests on single lap joint (SLJ) specimens are presented. Parameters from the FM experiments are used to define a FM-based crack growth law, which is then used to predict the fatigue lifetime of the SLJ specimens in the second part of the paper. The third part of the paper deals with the prediction of fatigue lifetime using a damage mechanics approach. In the final part of the paper, both FM- and DM-based prediction results are compared and conclusions are drawn.

2. EXPERIMENTAL

2.1. Materials and Joint Preparation

Compound double cantilever beams (CDCB) were used to generate fracture mechanics data in order to avoid the plastic deformation seen when testing double cantilever beams (DCBs) made from the unreinforced aluminium alloy sheet used in this work.

The procedures proposed by Blackman and Kinloch [15] were generally followed in the testing of the CDCBs in this work. Figure 1 shows the dimensions of the CDCBs. Two different adherend materials were used in the CDCB specimens. The actual joints to be tested were made from aluminium alloy 7075 T6 and FM 73 M epoxy film adhesive (Cytec Engineered Materials, Wrexham, UK). These joints were bonded to

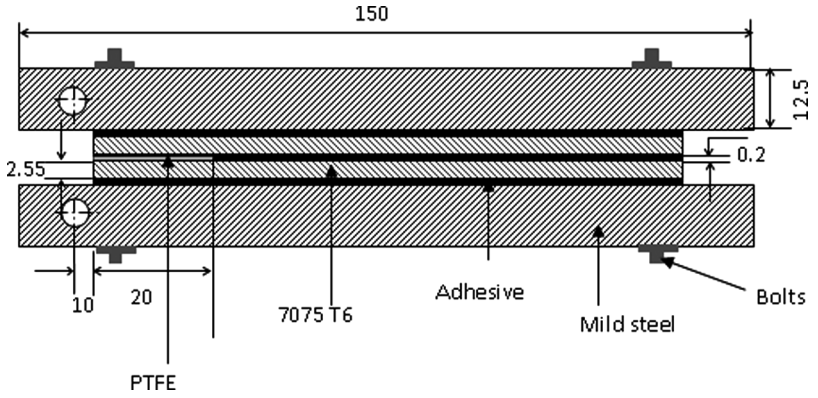

FIGURE 1 Compound double cantilever beam (dimensions in mm).

mild steel supporting adherends, also with FM 73 M adhesive. The 7075 T6 adherends were cleaned in an ultrasonic acetone bath for five minutes prior to pretreatment using an "AC DC" anodisation process [16]. This treatment is proposed as an environmentally friendly alternative to current chromate-containing pretreatments. In this pretreatment, the adherend to be bonded is one of the electrodes in an electrochemical cell. A weak mixture of phosphoric and sulphuric acid (5%) is used as the electrolyte and titanium as the other electrode. An alternating current (AC) is ramped up to 15 V over a period of 1 min and then kept at this voltage for 2 more mins. Thereafter, the current is changed to direct current (DC) and ramped to 20 V. The bath is kept at this voltage for a further 10 mins. The specimens are then washed with distilled water and dried using a hot air dryer. This pretreatment results in a duplex oxide layer film, approximately 1.9 μm thick, over the adherend surface. The film has an open, porous morpohology at the surface to enable wetting and interpenetration, and is denser adjacent to the metal interface to provide better corrosion protection. After the AC DC pretreatment, a thin film of BR 127 corrosion resistance primer (Cytec Engineered Materials, Wrexham, UK) was applied to the 7075 T6 adherends. This was dried at room temperature and then heated to 120°C for half an hour. The adherends were returned to room temperature before bonding with FM 73 M adhesive. The adhesive was cured at 120°C for 1 hour, with light pressure applied to the joints during curing as specified in the manufacturer's curing instructions.

A procedure recommended in Adams *et al.* [17] was used for pretreating the mild steel adherends used in the CDCBs. Any rust or mill scale was first removed using a clean wire brush and the samples were vapour degreased to remove any oil from the surface. The surface

was grit-blasted to make it more even and to remove any remaining rust. The specimens were then etched in an acidic solution for 10 min at 71–77°C, where the etching solution consisted of sodium dichromate (9%), sulphuric acid (22%), and water. During the etch, a magnetic stirrer was used to keep the concentration constant throughout the solution. After the specimens were etched, they were washed in a running stream of water and carbon residues were removed using a Nylon® brush. Subsequently, the surface was washed with distilled water followed by a bath of acetone and finally dried at 93°C using an air dryer. BR 127 primer was applied to the surfaces to be bonded, as described previously, before storing the specimens in a desiccator.

The CDCBs were prepared by first manufacturing the 7075 T6-FM73 DCBs and then retrofitting the DCBs with the supporting mild steel adherends to make the CDCBs. PTFE film was placed between the 7075 T6 adherends to create a pre-crack, as shown in Fig. 1. Extra bolted retrofittings were used to join the steel to the aluminium at both ends in order to prevent crack initiation between the steel and aluminium adherends. The joints used for fatigue testing were fitted with crack gauges supplied by Rumul GmbH (Rumul Russenberger Prufmaschinen AG, Neuhausen am Rheinfall, Switzerland) for crack growth monitoring. Before bonding the crack gauges to the CDCBs, any adhesive spew at the edges of the joint was removed to make an even surface. M-bond adhesive, provided by Vishay Instruments Plc. (Vishay Measurements Group, Basingstoke, UK) was used for bonding the gauges to the CDCBs. Electrical wires were soldered onto the gauges and connected to insulator bases mounted on the mild steel adherends. Lead wires from the insulator bases were then connected to the "Fractomat," which is a conditioner for the crack gauges supplied by Rumul GmbH.

Fatigue-life tests were carried out using adhesively bonded single lap joints (SLJs), following the protocol in BS ISO (4587:2003). As with the CDCBs, aluminium alloy 7075 T6 was used as the adherend material and FM 73 M epoxy film as the adhesive. The ACDC surface pretreatment used for the CDCB aluminium adherends was also used for the SLJs. The dimensions of the SLJs used are given in Fig. 2. The adhesive was cured at 120°C for 1 hour with a constant pressure applied through clips. The bonded joints were stored in a dessicator at room temperature prior to testing.

2.2. Testing

The CDCBs were tested quasi-statically using an Instron 6024 servo hydraulic testing machine (Instron, High Wycombe, UK). The tests were conducted under ambient laboratory conditions, with temperature

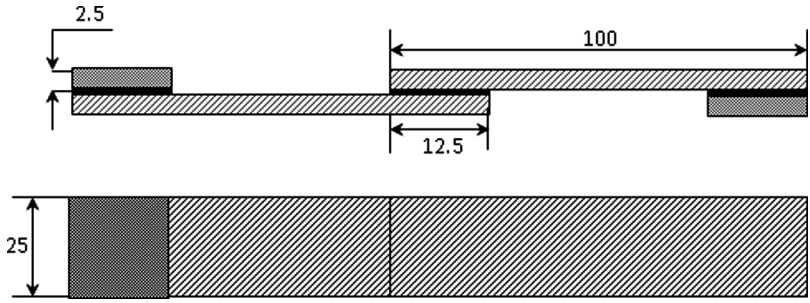

FIGURE 2 Single lap joint (dimensions in mm).

ranging from 22–25°C and with relative humidity ranging from 40–50%. A constant displacement rate of 0.1 mm/min was applied during the test. The edges of the CDCBs were polished and painted with white correction fluid in order to facilitate the monitoring of crack growth during the test. SLJs were also tested quasi-statically with a constant displacement rate of 0.1 mm/min and the same ambient conditions as those used for the CDCBs.

CDCBs were fatigue tested in displacement control, with a displacement ratio and frequency of 0.1 and 5 Hz, respectively, and a sinusoidal waveform. Displacement control is generally preferred in these tests as this results in a decreasing strain energy release rate as the crack grows, creating more stable crack growth and the generation of data over a wide range of strain energy release rates, including the fatigue threshold. Crack gauges were mounted on the edges of the CDCBs in order to measure crack growth during testing. SLJs were fatigue tested under load control with a load ratio of 0.1 and frequency of 5 Hz, as previously reported by Shenoy *et al.* [9]. Testing in load control is needed for the generation of load-life plots and if a unique relationship between strain energy release rate range (ΔG) and fatigue crack growth rate (FCGR) is assumed (as it commonly is), the data from the displacement control CDCB tests can be used to predict the fatigue life of the SLJs tested in load control. If, as was suggested by Ashcroft [8], previous load history has an effect on the relationship between ΔG and FCGR, then the fact that ΔG increases with crack length in the load control-tested SLJ and decreases with crack length in the displacement control-tested CDCB may affect the applicability of this approach. However, in this case, this effect is likely to be a lot smaller than that observed after the introduction of overloads by Ashcroft [8]; moreover, as this is the currently accepted method of using fracture mechanics data to predict fatigue failure in bonded joints, it is a useful comparison with the continuum

damage mechanics approach proposed in this paper. Different percentages of the quasi-static failure load (QSFL) were taken as the maximum load in the fatigue spectrum. All the fatigue tests were conducted under ambient laboratory conditions, as indicated previously.

3. FINITE ELEMENT MODELLING

3.1. Finite Element Mesh

Six-noded triangular elements (Element 125 in MSC Marc, MSC Software Corp., Santa Ana, CA, USA) were used for the lifetime prediction modelling, with both the FM and DM methods. This element was used to simplify the re-meshing procedure and to reduce the time needed to do so. In the case of bonded joints, the thickness of the adhesive layer is much smaller than the other dimensions in most cases; hence, for all the modelling in this paper, plane strain elements were used. Both material and geometric nonlinearity were accounted for in the analysis. Typical meshes taken from finite element models of a SLJ (both FM- and DM-based models) are shown in Fig. 3. A mesh sensitivity analysis was carried out, which is discussed in the results section.

3.2. Boundary Conditions

The set of boundary conditions applied were such that rigid body motion was suppressed. For the SLJ model, rotational symmetric conditions were used, enabling only half of the joint to be modelled and thereby saving in computation time. This model represented symmetric crack growth. In experimental tests it was seen that in many cases, near symmetric crack growth was seen; however, markedly asymmetric crack growth was also observed. As the manufactured SLJs were assumed to all be identical in the modelling then this variation in crack growth could not be predicted and the creation of models for each individual joint was not feasible. The approach taken is, hence, a pragmatic one in developing a generally applicable predictive methodology; however, the influence of crack path on predicted cycles to failure would be a useful future exercise. In addition, the joint was constrained in the vertical direction at the loaded end of the joint, as shown in Fig. 4.

3.3. Material Properties

Nonlinear material properties were used in all the models except those used in the FM-based prediction. The Young's moduli for adhesive, aluminium adherends, and mild steel were 2, 70, and 210 GPa,

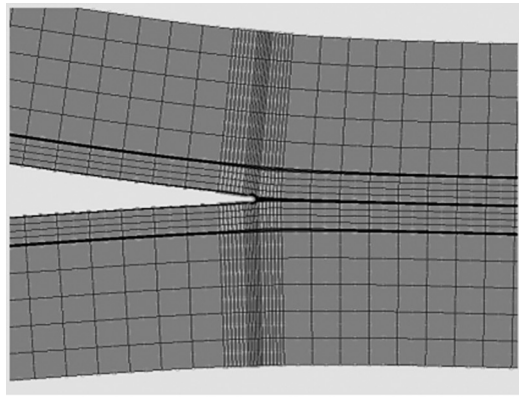

(a)

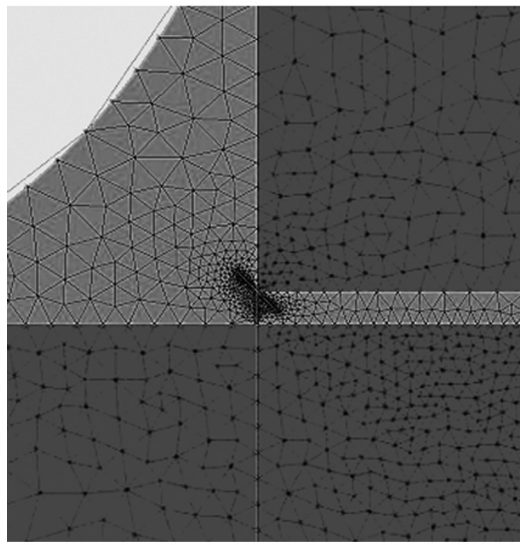

(b)

FIGURE 3 Typical finite element meshes used for (a) CDCB and (b) SLJ (showing high mesh density in the area of propagating crack).

respectively. The Mohr-Coulomb model used for the adhesive and linear elasticity was assumed for the adherends as no plastic deformation was observed in the adherends during the experiments. In the Mohr-Coulomb model the yield envelope, which is parabolic, is given by:

$$f = \left(3J_2 + \sqrt{3}\beta\sigma_{yp}J_1\right)^{(1/2)} - \sigma_{yp}. \quad (1)$$

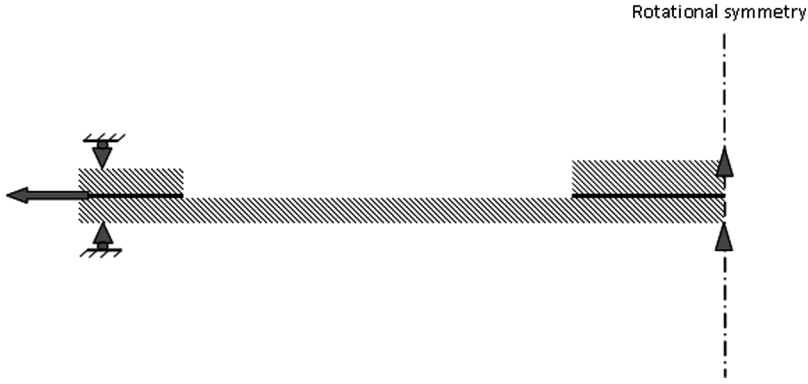

FIGURE 4 Boundary conditions used for SLJ simulations.

J_1 and J_2 are matrices defined as:

$$J_1 = \sigma_{ii} \tag{2}$$

$$J_2 = (1/2)\sigma_{ij}\sigma_{ij}, \tag{3}$$

where i, j = 1, 2, 3. The values for tensile yield stress, σ_{yp}, and the constant, β, were determined from experimental stress *versus* strain plots. Typical stress *vs.* strain plots for both tensile and compressive loading are shown in Fig. 5. It can be seen that there is a higher value of yield stress in compression than in tension. This difference in behaviour can

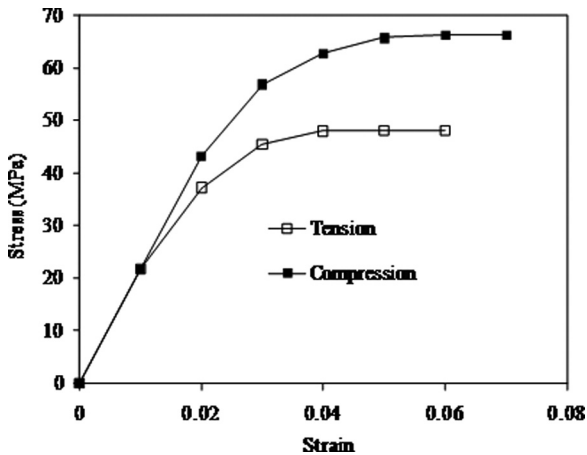

FIGURE 5 Typical stress *vs*. strain plots for FM 73 adhesive (Jumbo [18]).

be represented using the parabolic Mohr-Coulomb model described above. The experimental details for determining the stress strain plots are described in Jumbo [18]. The tensile yield stress was equal to 28.73 MPa and a value of 0.001057 was used for β.

4. THEORY AND ALGORITHMS

4.1. Determination of Mode I Strain Energy Release Rate (G_i)

The results from the CDCB quasi-static tests were used to determine the critical strain energy release rate, G_{IC}, using the linear elastic fracture mechanics (LEFM) equation:

$$G_{IC} = \frac{P_C^2}{2b}\frac{dC}{da}, \tag{4}$$

where P_C is the failure load, b is the width of the specimen, C is the compliance of the specimen, and a is the crack length. dC/da in Eq. (4) can be determined by fitting a curve to an experimental C vs. a graph. This is termed the experimental compliance (EC) method. The results from the fatigue testing of the CDCBs were used to relate G_I to crack growth rate, da/dN.

4.2. Lifetime Prediction Using the FM Based-Approach

The results from the CDCB experiments were used to determine the fatigue lifetime of SLJs using a FM approach. In this approach, the fatigue crack growth rate was defined using a Paris-type crack growth law [19]. This law is characterised by two constants, which were taken from the tests on the CDCB samples. The Paris-type law used was:

$$\frac{da}{dN} = C(\Delta G)^n. \tag{5}$$

The ΔG value needed to be greater than a threshold value, ΔG_{th}, for crack growth to occur and immediate failure was assumed to take place when G_{max} equalled G_{IC}. Equation (5) was numerically integrated to determine the number of cycles to failure under fatigue loading. This procedure was programmed in a Python® (Python Software Foundation Inc., Hampton, New Hampshire, USA) script, which acted as an external interface to the MSC Marc FEA software. The value for G was determined using the virtual crack closure technique (VCCT) available in MSC Marc software. The G value determined here was the sum of G_I and G_{II} ($G_T = G_I + G_{II}$) which was used to define the mixed mode criterion in the simulation of the SLJs. The value of ΔG

in Eq. (5) is given by:

$$\Delta G = G_{max} - G_{min}, \tag{6}$$

where G_{max} and G_{min} are the maximum and minimum values of G, determined at the maximum and minimum loads of the fatigue loading spectrum, respectively. The algorithm used in the finite element implementation of the numerical crack growth integration (NCGI) is shown in Fig. 6. The algorithm can be described in the following steps:

Step 1: Model the SLJ with an initial crack length, a_o, and set the number of cycles, N, equal to zero.
Step 2: Perform quasi-static analysis for both maximum fatigue load L_{max} and minimum fatigue load L_{min}.
Step 3: Determine G_{max}, G_{min}, and ΔG using VCCT. If $G_{max} > G_{IC}$, N equals the number of cycles to failure, N_f. If $G_{max} < G_{th}$, there is no crack growth.
Step 4: Calculate the fatigue crack growth rate da/dN using Eq. (5).
Step 5: Calculate the number of cycles using:

$$N_{i+1} = N_i + \frac{da}{da/dN}, \tag{7}$$

where da is a selected crack growth increment.
Step 6: Check if $a_i = a_f$, where a_f is the crack length prior to fast crack growth. If yes, then $N = N_f$. If no, then increase the crack length by da using:

$$a_{i+1} = a_i + da. \tag{8}$$

This procedure is repeated for different fatigue loads and the N_f values calculated for all the fatigue loads.

4.3. Lifetime Prediction Using DM-Based Approach

In this section, the DM approach, which was used to simulate damage evolution prior to crack growth, is described. Damage prior to macro crack formation was simulated using the damage growth law:

$$\frac{dD}{dN} = m_1(\epsilon_p)^{m_2}, \tag{9}$$

where ϵ_p is the equivalent plastic strain and m_1 and m_2 are constants determined *via* experiments. The damage law was implemented using

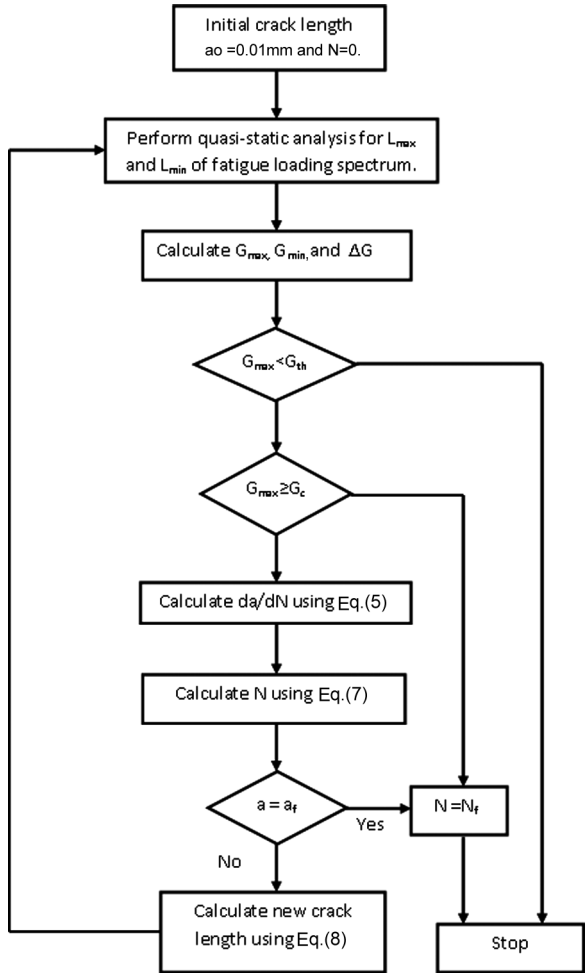

FIGURE 6 NCGI algorithm used for lifetime prediction using FM approach.

a Python script, which acted as an interface to the MSC Marc software. The algorithm used to simulate the damage and crack growth in SLJs using the DM approach is given in Fig. 7. This can be described in the following steps:

Step 1: A SLJ model is built using MSC Marc software with the material properties given in Section 3.3. The values for number of cycles, N, and damage, D, are set to zero.

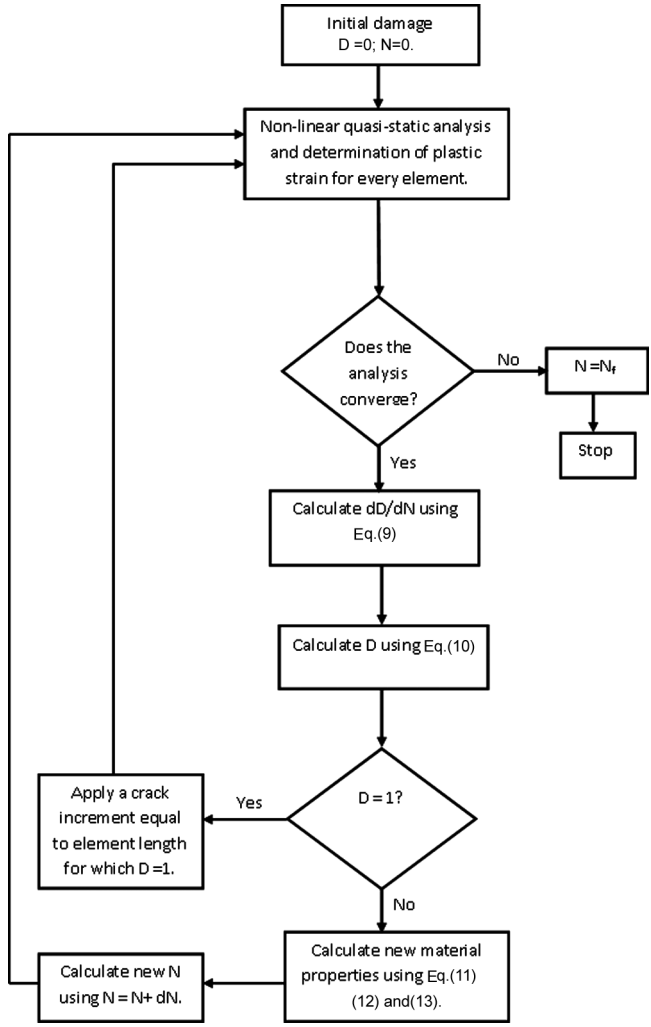

Figure 7. Algorithm used for lifetime prediction using DM approach.

Step 2: A non-linear static analysis is carried out and plastic strain is determined for all the elements in the adhesive layer.
Step 3: Check if the analysis converges; if yes then Step 4, otherwise $N = N_f$ and stop the program.
Step 4: The damage rate dD/dN is then determined for each element in the adhesive using Eq. (9).

Step 5: Damage is calculated using the damage rate determined in the last step using:

$$D_{i+1} = D_i + \frac{dD}{dN} dN, \tag{10}$$

where dN is the selected increment to the number of cycles.

Step 6: Check if $D = 1$; if yes then apply a crack increment equal to the length of the element for which $D = 1$ and re-mesh to obtain a fine mesh at the crack tip. Go to Step 2.

Step 7: If $D \neq 1$, then for the new value of damage, calculate new material properties as:

$$E = E_0(1 - D) \tag{11}$$

$$\sigma_{yp} = \sigma_{yp0}(1 - D) \tag{12}$$

$$\beta = \beta_0(1 - D), \tag{13}$$

where E_0, σ_{yp0}, and β_0 are Young's modulus, yield stress, and the plastic surface modifier constant for the Parabolic Mohr-Coloumb model, respectively (as determined from tensile and compressive stress-strain testing of bulk adhesive samples). Calculate new value of N, go to Step 2, and repeat.

The constants m_1 and m_2 were determined by repeating the procedure above for different values at two different fatigue loads and optimising. These constants were then kept constant to determine the life for other fatigue loads. In this way, m_1 and m_2 were used to characterise completely the mechanism of fatigue damage and failure of the SLJs.

5. RESULTS AND DISCUSSION

5.1. Quasi-Static and Fatigue Testing Results

An average QSFL of 11.95 kN was found for the five SLJ samples tested, with a standard deviation (SD) of 0.31 kN. The fracture surfaces exhibited predominantly cohesive failure in the adhesive, thus demonstrating the effectiveness of the environmentally friendly ACDC surface pretreatment. The fatigue test data for the SLJs is given in Fig. 8, where the maximum fatigue load is plotted against the number of cycles to failure. It can be seen that there is an approximately linear increase in the log of cycles to failure with decrease in maximum fatigue load.

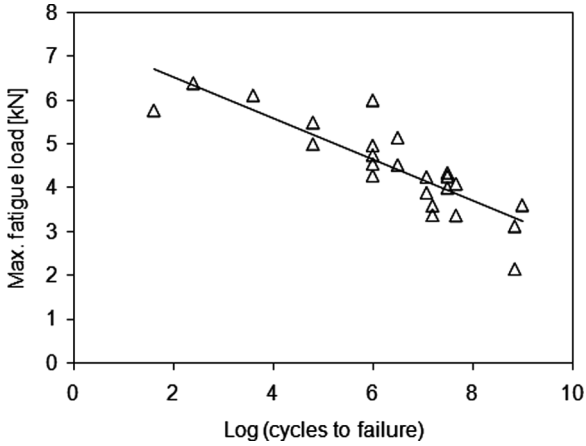

FIGURE 8 L-N curve for SLJs with aluminium 7075 T6 adherend and FM 73 adhesive.

5.2. Determination of G_{IC}

As described in Section 4.1, G_{IC} was calculated using the EC method. Experimental values for dC/da were used in Eq. (4), with corresponding values of failure load, P_C, in order to determine G_{IC} at different crack lengths. The G_{IC} values were found to be approximately independent of crack length, with a mean value from five tests of $2695\,J/m^2$ and standard deviation of $212\,J/m^2$. The scatter can be attributed to the variability of the material microstructure and manufacturing defects, such as voids, that are always seen in these joints. The value of G_{IC} varies with crack length for each sample, as well as between samples, and the complex and varying crack path produces a degree of variability in these samples.

5.3. Determination of Fatigue Crack Growth Law

The Mode I fatigue crack growth rate was also determined using CDCB specimens.

Figure 9(a) shows the variation of measured crack length with number of cycles during one of the fatigue tests. It can be seen that the rate of crack growth decreases as the number of cycles increases. This type of plot was used to calculate the fatigue crack growth rate, da/dN, as a function of crack length. Figure 9(b) shows an example of the rate of change of compliance with crack growth, dC/da, as a function of cycles. It can be seen that dC/da decreases nonlinearly with the number of cycles.

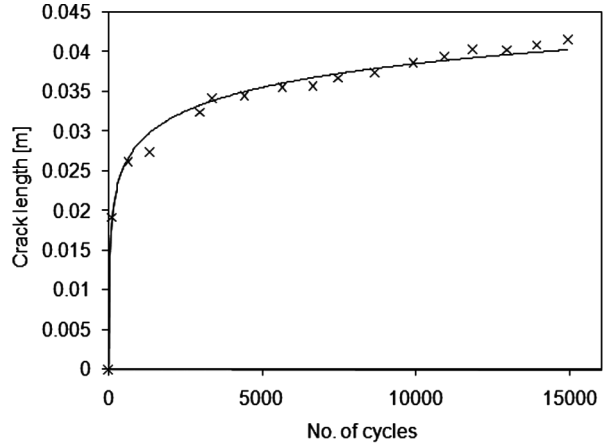

(a)

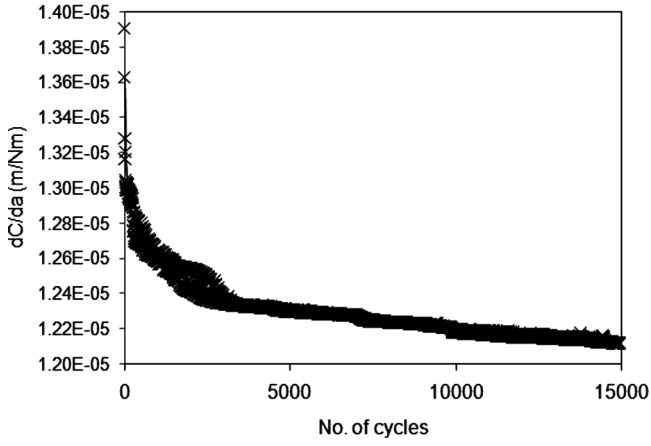

(b)

FIGURE 9 (a) Crack plotted against number of fatigue cycles, (b) rate of change of compliance with crack length plotted against number of cycles.

G values for fatigue were calculated using Eq. (4), where the values of dC/da were taken from Fig. 9. Figure 10 shows crack growth rate plotted against G_{max}. The plot illustrates three regions, as observed by previous workers, *i.e.*, a threshold region below which there is no crack growth, a Paris-type law region, where log da/dN is approximately proportional to log G_{max}, and a rapid increase in slope approaching G_{IC}. The experimental data can be represented quite well

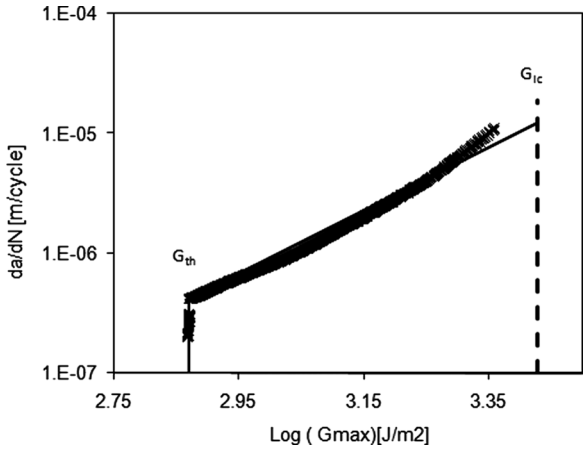

FIGURE 10 Logarithmic plot of fatigue crack growth rate against strain energy release rate.

by a straight line fit between the limits of G_{th} and G_{IC}. In some cases a more complex sigmoidal fit [20] to such data is proposed; however, in this case, the simpler straight-line fit was seen to provide equally good lifetime predictions. This curve represents the characteristic fatigue behaviour under fatigue loading for the FM 73 M adhesive and can be used in lifetime prediction for different types of adhesive joints. However, care has to be taken to ensure that fracture conditions are similar to those seen in the CDCB and a suitable mixed mode fracture criterion must be used if fracture is not pure Mode I. In this paper, the mixed mode criterion, G_T, was determined by linearly adding the G_I and G_{II} components determined in the FEA software. A more comprehensive approach is to test over a range of mode mixity and fit an appropriate function to the data; however, the extra effort required in the testing (often for little added benefit) means that the approach used here is the one commonly used. The fitted experimental curve in this case gave the following crack growth law:

$$\frac{da}{dN} = 3.5 \times 10^{-16}(\Delta G)^{3.2}. \tag{14}$$

5.4. Lifetime Prediction Using FM Approach

Crack growth in the SLJs was simulated using FM to predict the fatigue lifetime. The crack growth direction was chosen as perpendicular

to the direction of maximum principal stresses ahead of the crack tip. Figure 11 shows the resultant crack path schematically (a), which is in agreement with that seen experimentally (b). A mesh sensitivity analysis was conducted to decide on the required element length in the crack tip region to obtain a mesh-independent G value. Convergence was obtained with an element length of 0.02 mm.

In Fig. 12(a) crack length is plotted against number of cycles for both experimental measurements and FM-based predictions for a fatigue load of 63% of QSFL. The experimental crack length curves are taken from Shenoy *et al.* [21] and details of the experimental procedures used to measure crack length can be found in that paper. It can be seen that crack growth is stable until approximately 1500 cycles, after which the crack growth accelerates. Towards the end of the fatigue life, the curve becomes vertical, implying a quasi-static type of crack growth. It can be seen that there is a tendency for an under-prediction of the

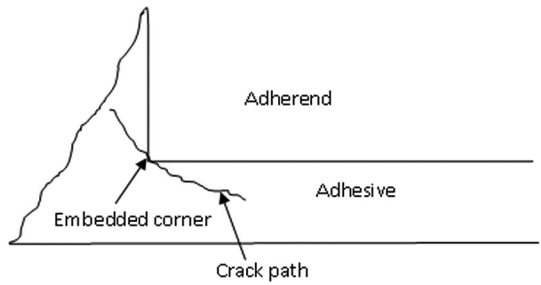

(a)

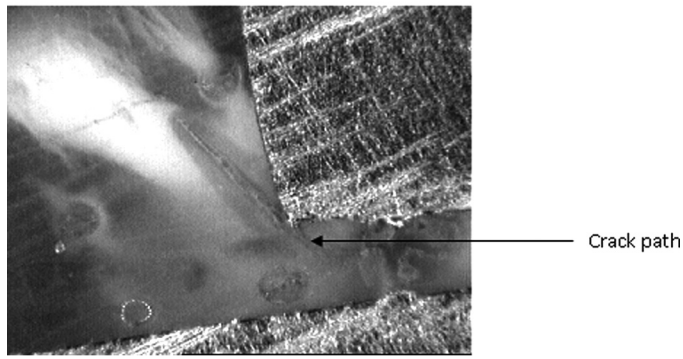

(b)

FIGURE 11 Crack path during fatigue loading shown (a) schematically and (b) optical micrograph of polished sample section.

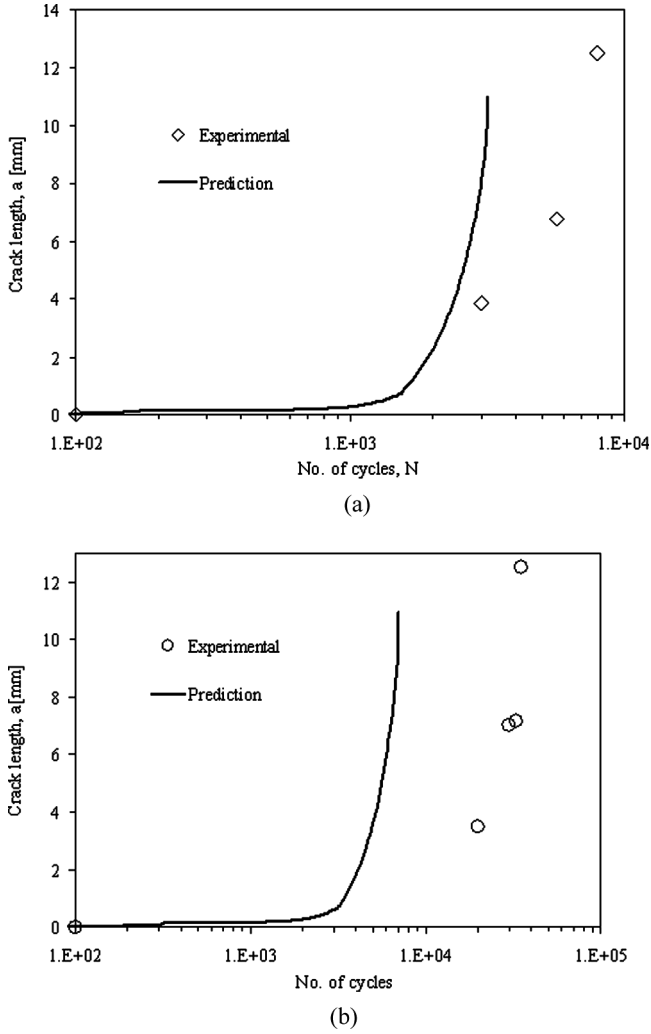

FIGURE 12 Fatigue crack growth rate comparison between experimental and FM-based prediction for the max. fatigue load of (a) 63% of QSFL and (b) 54% of QSFL.

experimental crack length. This is even more evident with a fatigue load of 54% of QSFL, as shown in Fig. 12(b). The difference between the experimental and predicted crack growth can be attributed to the fact that as the fatigue load decreases, crack initiation domination in the fatigue lifetime increases, as described by Shenoy *et al.* [9]. The FM-based approach does not consider the crack initiation phase that

may exist prior to crack growth in adhesive joints. The initiation phase has the effect of delaying the crack growth phase, especially at low loads, which explains the discrepancy between experimental and predicted crack lengths seen in Fig. 12(b). Although some scatter was seen in the fatigue life of the joints, the major trends described above were seen in all the samples examined.

Total G (G_T) is plotted against number of cycles for the SLJ samples in Fig. 13, where G_T is the linear sum of Mode I and Mode II values for G. As described previously, G was calculated in the MSC Marc software using the VCCT technique for both Modes I and II. It can be seen that G_T increases rapidly with cycles towards the end of the fatigue life, in a similar fashion to crack growth. This tendency is the same for all fatigue loads.

A sensitivity check was conducted for the number of cycles to failure (N_f) with respect to the initial crack length, a_o. It was seen that with initial crack lengths over 0.08 mm, the predicted N_f starts to decrease. For all the analyses, an initial crack length of 0.01 mm was selected to ensure the predicted fatigue life was independent of initial crack length. The location of the initial crack was at the embedded adherend corner, as seen in experimental observations [9].

The maximum fatigue load is plotted against the logarithm of the number of cycles to failure for the FM-based prediction and the experiments in Fig. 14. It can be seen that the FM-based approach

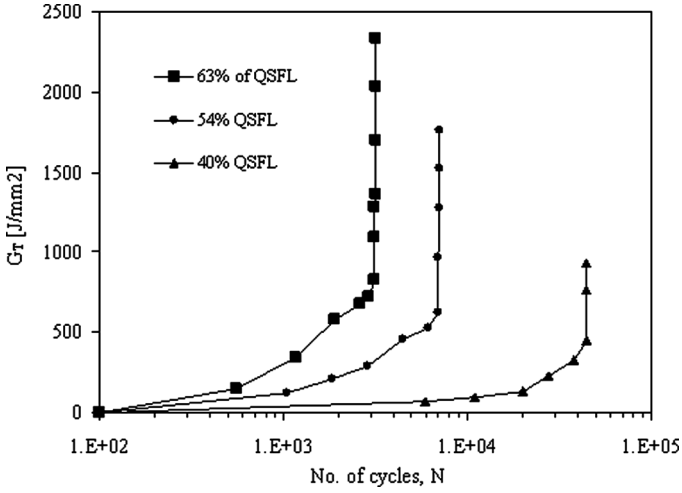

FIGURE 13 Variation of G_T with respect to number of cycles for various maximum fatigue loads.

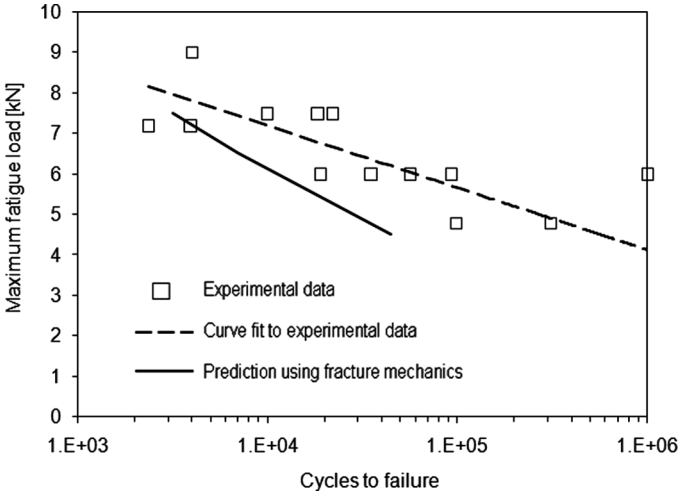

FIGURE 14 Comparison between experimental and FM-based fatigue lifetime prediction.

predicts the fatigue life well at high fatigue loads, however, at lower fatigue loads; this approach under-predicts the fatigue life. Hence, as the fatigue load decreases, the gap between experiment and prediction increases. This indicates that the FM-based prediction method cannot be accurately used when the fatigue life is dominated by crack initiation rather than crack propagation. A more advanced approach, wherein the damage prior to crack growth is also predicted, is needed in this case. This is discussed in the next section.

5.5. Lifetime Prediction Using DM Approach

Plastic strain was used as the parameter for damage progression in this approach as this is a convenient method of introducing a level of strain below which damage does not occur. The adhesive layer was progressively damaged according to the constitutive law defined in Eq. (9). Prior to determining the optimal values for the constants defined in this equation, a sensitivity analysis was conducted with respect to the number of cycles increment parameter, dN. It was found that a value of dN of 100 cycles was optimal, as discussed in [22].

Figure 15 shows example stress *vs*. strain diagrams, calculated for degraded material using Eqs. (11)–(13). It can be seen that as the material is degraded, both elastic and plastic regions of the material are adjusted. The damage in this graph is defined as the difference

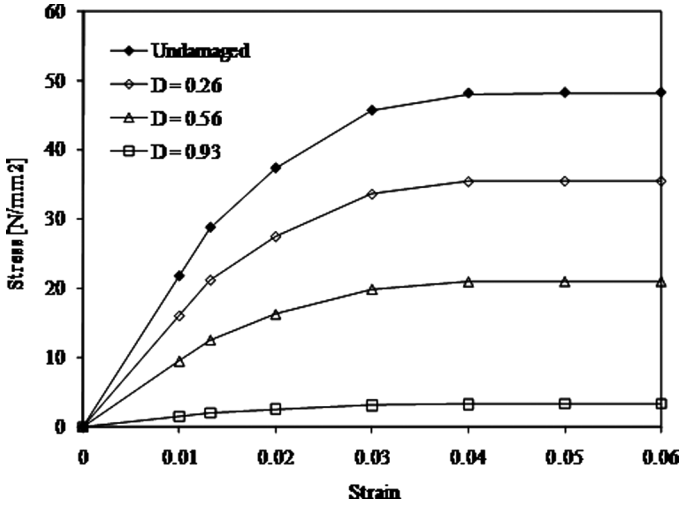

FIGURE 15 The effect of the damage parameter on the calculated adhesive stress-strain behaviour.

between the undamaged curve and that of the damaged material. The plastic strain for one of the elements in the adhesive layer near the embedded corner is plotted against the number of cycles in Fig. 16. It can be seen that initially the strain increases in a stable manner and then rises at a much faster rate towards the end of the fatigue life. A comparison of plastic strain distribution with experimentally observed damage in [9] showed a close match in terms of the location and extent of the high strain region and the visually observed damaged region. This provides some validation for the use of equivalent plastic strain in the damage law.

Damage calculated in an element near to the embedded corner prior to macro-cracking is plotted against the number of cycles in Fig. 17. It can be seen that for all fatigue loads the damage progression shows a similar tendency. Once the crack initiates, there is an accelerating crack growth, leading to failure. This is because the average damage calculated over the entire adhesive is increasing rapidly once crack growth has started. The average damage value for all the elements in the adhesive layer is plotted against the number of cycles for a maximum fatigue load of 54% of QSFL in Fig. 18. It can be seen that, towards the end of the fatigue life, the average damage increases rapidly indicating a fast crack growth. The damage value is not equal to one here, because even after the final fracture, there will be a portion of adhesive (elements in FE mesh) which is undamaged or only partially damaged.

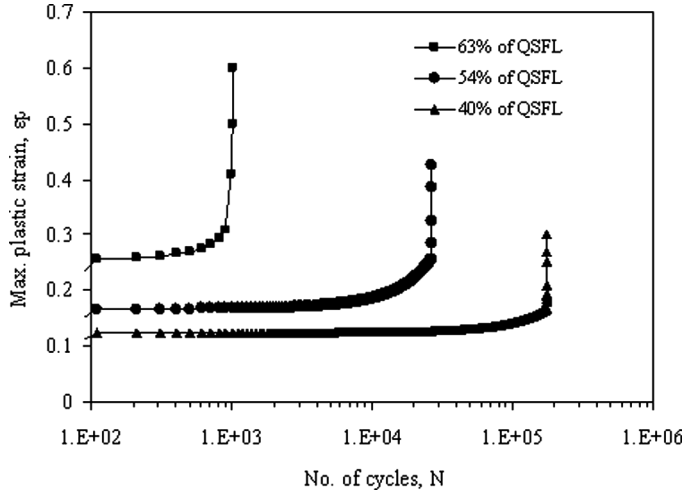

FIGURE 16 Maximum plastic strain plotted against number of cycles for an element in the damage initiation region.

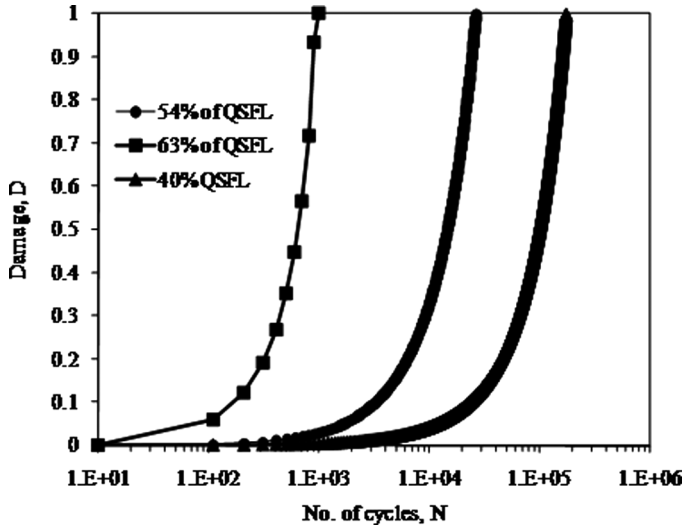

FIGURE 17 Damage progression in SLJ for different fatigue loads simulated using the DM approach.

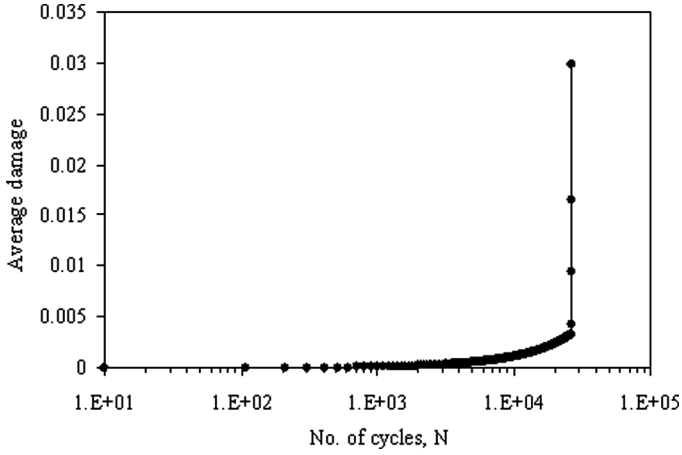

FIGURE 18 Average damage in the adhesive for maximum fatigue load of 54% of QSFL.

A comparison between DM predicted and experimentally measured fatigue lives is made in Fig. 19. An excellent prediction can be seen for all fatigue loads. The constants used for the damage rate law, m_1 and m_2 were 8 and 7, respectively, for this prediction.

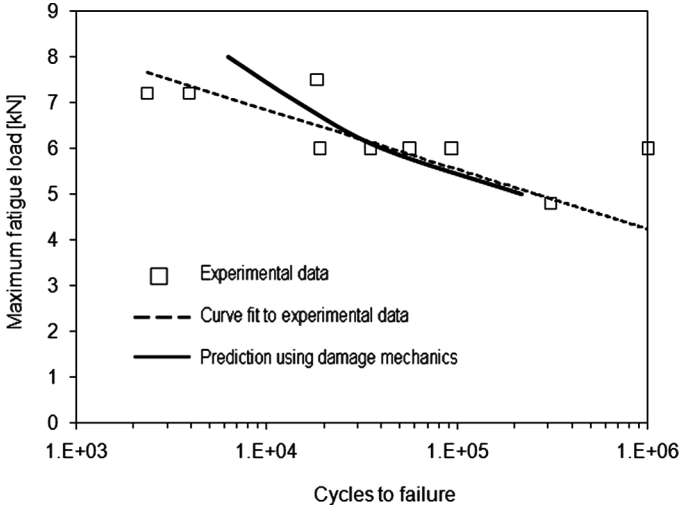

FIGURE 19 Comparison between experimental and DM prediction of fatigue lifetime ($m_1 = 8$, $m_2 = 7$).

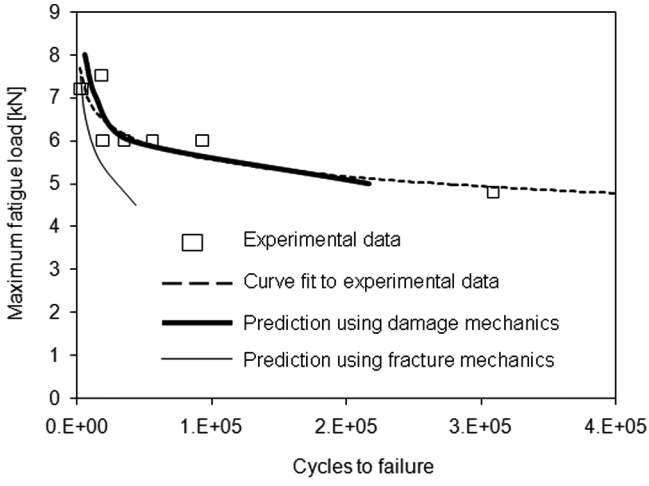

(a)

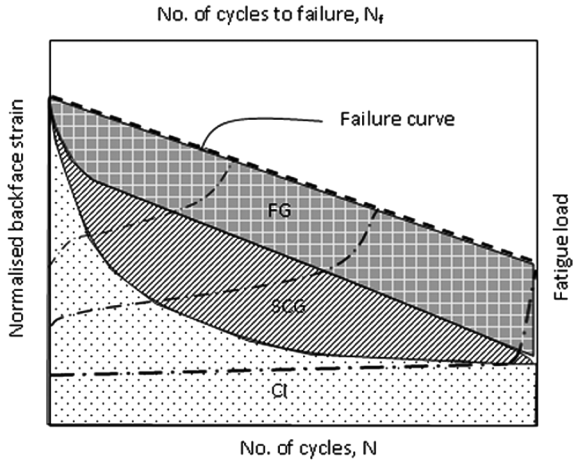

(b)

FIGURE 20 (a) Comparison between experimental, FM-, and DM-based fatigue lifetime; (b) damage progression model (Shenoy *et al.* [9]).

5.6. Comparison Between FM and DM Approaches

A comparison is made in Fig. 20(a) between the FM and DM approaches for fatigue lifetime prediction. It can be seen that the accuracy of the FM prediction is load-dependent whereas the DM prediction is not. The reason that the FM approach under-predicts the

fatigue life at lower loads is that the fatigue life is dominated by crack initiation, as described by Shenoy *et al.* [9]. Their damage progression model is shown in Fig. 20(b). In this figure, normalised backface strain (BFS) is plotted against number of cycles and maximum fatigue load is plotted against the number of cycles to failure. It can be seen that the fatigue lifetime consists of three regions; crack initiation denoted as CI, a stable crack growth region, denoted by SCG, and a fast crack growth region, denoted by FG. At lower fatigue loads, the fatigue life is dominated by crack initiation with crack growth only occurring towards the end of the fatigue life. As the DM approach takes into consideration the damage evolution prior to cracking, it predicts the lifetime well under all fatigue loads

6. DISCUSSION AND CONCLUSIONS

For the adhesively joined SLJs used in this work, it was seen that a FM-based approach could only accurately predict the fatigue life at higher fatigue loads. At lower loads, the fatigue life is under-predicted because crack initiation dominates the fatigue life and is not accounted for in the fracture mechanics analysis. This could potentially be corrected for by determining the fatigue initiation life, *e.g.*, by using the method proposed by Lefebvre and Dillard [10]; however, this would take considerable extra experimentation. An alternative is to use damage mechanics (DM) and, in this work, it was seen that plastic strain could be used as a simple and effective parameter to characterise the pre-crack damage evolution in bonded joints through a simple power law. The DM-based approach predicted the fatigue life well at both lower and higher fatigue loads because it was able to predict both damage initiation and crack growth. It should be noted that a cohesive zone model [23,24] would also be able to predict both initiation and propagation of fatigue damage; however, drawbacks in this case would be that the crack path would have to be pre-defined and that damage would be restricted to the path of the cohesive zone elements.

There is merit in all the progressive damage models discussed above. The traditional fracture mechanics approach is a simple and powerful method of predicting crack propagation in relatively brittle materials where damage is restricted to the crack tip. The cohesive zone model can be seen as an extension of this method, enabling damage initiation and damage in the crack path to be modelled. The continuum damage method, such as that described in this paper, is more suited to a more widespread damage scenario, such as that seen in more ductile materials. The limits of applicability of the simple

power law model based on equivalent plastic strain is yet to be determined; however, it is suggested that the method, or variations on it, should be considered as a serious alternative means of modelling fatigue damage in bonded joints, particularly in cases of widespread damage. This method can also be readily extended to variable amplitude fatigue, as discussed in Shenoy *et al.* [22].

REFERENCES

[1] Ashcroft, I. A. and Crocombe, A. D., Modelling Fatigue in Adhesively Bonded Joints *Modelling of Adhesively Bonded Joints*, L. F. M. da Silva and A. Oechsner (Eds.) (Springer, Berlin, 2008), Ch. 7, pp. 183–223.
[2] Gorden, K., *J. Comp. Struct.* **72**, 119–129 (2006).
[3] Palmgren, A., *Vereins Deutscher Ingenieure* **68**, 339–341 (1924).
[4] Miner, M. A., *J. Appl. Mech.* **67**, A 159-A 164 (1945).
[5] Erpolat, S., Ashcroft, I. A., Crocombe, A. D., and Abdel-Wahab, M. M., *Int. J. Fat.* **26**, 1189–1196 (2004).
[6] Schaff, J. R. and Davidson, B. D., *J. Comp. Mater.* **31**, 158–181 (1997).
[7] Abdel Wahab, M. M., Ashcroft, I. A., Crocombe, A. D., and Smith, P. A., *Compos. Part A.* **35**, 213–222 (2004).
[8] Ashcroft, I. A., *J. Strain Anal.* **39**, 707–716 (2004).
[9] Shenoy, V., Ashcroft, I. A., Critchlow, G., Crocombe, A. D., and Abdel Wahab, M. M., *Int. J. Adhes. Adhes.* **29**, 361–371 (2009).
[10] Lefebvre, D. R. and Dillard, D. A., *J. Adhes.* **70**, 119–138 (1999).
[11] Quaresimin, M. and Ricotta, A., *Int. J. Fat.* **28**, 1166–1176 (2006).
[12] June, W., *Eng. Fract. Mech.* **45**, 349–355 (1993).
[13] Taylor, M., Verdonschot, N. R. H., and Ziopos, P., *J. Mater. Sci.* **10**, 841–846 (1999).
[14] Abdel Wahab, M. M., Ashcroft, I. A., Crocombe, A. D., and Shaw, S. J., *J. Adhes. Sci. Technol.* **7**, 763–781 (2001).
[15] Blackman, B. R. K. and Kinloch, A. J., *Fracture Tests for Structural Adhesive Joints*, (Elsevier Science, Amsterdam, 2001).
[16] Critchlow, G., Ashcroft, I. A., Cartwright, T., and Bahrani, D., *Anodising Aluminium*, Patent no. GB 3421959A, (UK, 2005).
[17] Adams, R. D., Comyn, J., and Wake, W. C., *Structural Adhesives in Engineering*, (Chapman and Hall, London, 1997).
[18] Jumbo, S. F., Modelling of residual stresses and environmental degradation in adhesively bonded joints, Ph.D. thesis, Loughborough University, Loughborough, Leicestershire, UK (2007).
[19] Paris, P. and Erdogan, F., *J. Bas. Engin. Trans. ASME* **85** (Series D), 528–534 (1963).
[20] Ewalds, H. L., *Fracture Mechanics*, (Edward Arnold, London, 1984).
[21] Shenoy, V., Ashcroft, I. A., Critchlow, G., Crocombe, A. D., and Abdel Wahab, M. M., *Int. J. Fat.* **31**, 820–830 (2009).
[22] Shenoy, V., Ashcroft, I. A., Critchlow, G., and Crocombe, A. D., *Eng. Fract. Mech.* **77**, 1073–1090 (2010).
[23] Liljedahl, C. D. M., Crocombe, A. D., Wahab, M. A., and Ashcroft, I. A., *Int. J. Adhes. Adhes.* **27**, 505–518 (2007).
[24] De Moura, M. F.S. F., *Modelling of Adhesively Bonded Joints*, L. F. M. da Silva and A. Oechsner (Eds.) (Springer, Berlin, 2008), Ch. 6, pp. 155–182.